

# Engineering geological appraisal and preliminary support design for the Salarha Tunnel, Northeast Turkey

Ayberk Kaya<sup>1</sup> · Aytuna Sayın<sup>2</sup>

Received: 28 May 2017 / Accepted: 10 October 2017 / Published online: 27 October 2017  
© Springer-Verlag GmbH Germany 2017

**Abstract** The purpose of this study is to determine the engineering geological properties of the rock masses and to recommend a convenient support design for the Salarha Tunnel located in northeast Turkey. The detailed geotechnical studies were performed in three phases as surface, subsurface and laboratory studies to assess the rock masses that mainly consist of sedimentary and volcanic rocks. Empirical, analytical and numerical methods were combined for safe tunnel design. The RMR, Q and NATM systems were used as empirical methods to define the rock masses and to determine the preliminary support design. The convergence-confinement analytical method was utilized. The performance of the suggested empirical support design, extent of the plastic zones and deformations were analyzed by means of the finite element method (FEM)-based 2D and 3D numerical modeling. According to analytical and numerical analyses results, the empirical support design was sufficient to prevent stability problems developing around the rock masses surrounding the tunnel. The interpretations of results demonstrate that the 3D numerical method seems to fit even better with the respective outcomes from the analytical method. Thus, it is suggested that the empirical, analytical and numerical methods should be combined for a more reliable support design.

**Keywords** Tunneling · Rock mass classification systems · Convergence-confinement method · Finite element method · Tunnel support design

## Introduction

Determination of the most suitable and economical support design is highly applicable to tunnel project design and construction. In the early stages of tunnel design, designers base their estimations on previous experience, and commonly prefer to use empirical, analytical and numerical approaches (Lü et al. 2011; Zhang and Goh 2012, 2015; Goh et al. 2016, 2017). The rock mass rating (RMR), rock mass quality (Q) and New Austrian tunneling method (NATM) rock mass classification systems are used by many engineering geologists and tunnel engineers owing to their practicality. Although these empirical methods are useful tools in preliminary support design estimation, they do not ensure necessary information in stress and strain evaluation for tunneling. Therefore, the analytical methods are employed as a first estimation of the design parameters, providing guidance in the conceptual stage of the design process. A number of analytical methods are currently used for the design and analysis of tunnels considering the elastic or elasticoplastic models of material behavior (i.e. Muir-Wood 1975; Brown et al. 1983; Detournay 1986; Wang 1996; Carranza-Torres and Fairhurst 1999; Carranza-Torres 2004, 2009; Park and Kim 2006; Wang et al. 2014). Among them, the convergence-confinement method (Carranza-Torres and Fairhurst 1999, 2000) has played an important role in providing insight into the interaction between the lining support and the surrounding ground mass. This method is based on a concept that involves an analysis of the ground-structure interaction by independent studies of the behavior of the ground and of the tunnel support.

---

Submitted to "Bulletin of Engineering Geology and the Environment"

✉ Ayberk Kaya  
ayberk.kaya@erdogan.edu.tr

<sup>1</sup> Department of Geological Engineering, Faculty of Engineering, Recep Tayyip Erdogan University, 53100 Rize, Turkey

<sup>2</sup> 10th Division of Turkish General Directorate of Highways, 61310 Trabzon, Turkey

Due to the rapid advances in computer systems, numerical methods have gained popularity in determination of deformations and stress distributions, and control of the tunnel support design for the best solution. If empirical and analytical methods are integrated into numerical techniques, more realistic results in tunnel support design and stability analysis are obtained. The numerical analyses such as analytic element method (AEM), boundary element method (BEM), finite difference method (FDM), discrete element method (DEM) and finite element method (FEM) have been increasingly used today in geotechnical projects to control the validity of results obtained from empirical and analytical techniques. Since numerical methods consider the geometry of underground openings, in situ stresses acting on surrounding rocks and physico-mechanical/elastic parameters, they are powerful design tools in underground constructions. The DEM and FEM have become most preferred methods in tunnel applications by many researchers. The DEM is rapidly gaining in popularity for analyzing the behavior of tunnels excavated in jointed rock masses (i.e. Barton et al. 1994; Bhasin et al. 1996; Goodman 1995; Vardakos et al. 2007; Barla et al. 2013; Boon et al. 2015). The DEM is especially useful for kinematic studies of large block systems where highly jointed rock masses around the tunnel are modeled. The magnitude of block movements that can be analyzed is larger compared to that obtained from most continuum models. The computation requires the input of joint location and orientation. This information is not normally known prior to construction of the tunnel. Even so, parameter studies can be performed by assuming various joint configurations in the DEM. However, highly complex underground conditions and tunnel characteristics can be analyzed in the FEM. The capability of the FEM includes the simulation of complex constitutive laws, non-homogeneities and the impact of advance and time-dependent characteristics of the construction methods. At present, confidence in the obtained results is largely drawn from case histories to which the FEM had been applied successfully (i.e. Ozsan and Basarir 2003; Sari and Pasamehmetoglu 2004; Gurocak et al. 2007; Karakus et al. 2007; Basarir 2008; Ozsan et al. 2009; Solak 2009; Gurocak 2011; Kaya et al. 2011; Kaya and Bulut 2013; Akgun et al. 2014; Satici and Unver 2015; Yalcin et al. 2015; Agan 2016).

The Turkish General Directorate of Highways (KGM) decided to build a tunnel for a short connection between the Rize periphery and Kucukcayir government highways (KM: 0 + 000–4 + 289) due to the increasing traffic load and as a precaution to decrease traffic congestion in the coming years. The Salarha Tunnel is situated between KM: 0 + 200–3 + 150 (2.950 km). The tunnel will be constructed as a double-tube modified horse-shoe shaped tunnel using the conventional drilling-blasting and mechanical excavation methods depending on the existing ground conditions and behaviors. The planned span and height of the tunnel are 12 m and 9 m, respectively.

The overburden varies between 20 and 290 m. The location of the project is shown in Fig. 1.

In this study, empirical, analytical and numerical support procedures were applied to the Salarha Tunnel. An engineering geological investigation including field and laboratory studies followed by classification of rock masses using the RMR, Q and NATM systems was carried out to determine the support elements. Field studies consisted of geological mapping, drilling, scan-line survey and geotechnical description. The necessary preliminary support design was estimated by means of the empirical method. An analytical approach called the convergence-confinement method was used in order to determine the radial displacements for the unsupported tunnel case. In addition to the analytical method, 2D and 3D FEM analyses were undertaken in order to define the extent of the failure zones and total displacements developed around the tunnels. Furthermore, the performance of the empirical support design suggested by the Q system was controlled by the help of the numerical analyses.

In this context, based on the convergence-confinement analysis results, this paper compares and assesses the 2D FEM analysis results versus the 3D numerical analysis. The strengths and weaknesses of the 2D and 3D methods in design of the tunneling project were determined. Another aim of this study is to ensure a methodology in order to increase the confidence of tunnel engineers in the use of the 3D FEM method as a numerical tool for the prediction of tunnel behavior.

## Geological setting

Based on the lithological and structural evidence, the Eastern Pontides is subdivided into southern and northern zones (Ketin 1966). The study area is located in the northern part of the Eastern Pontides tectonic assembly in the Black Sea region of Turkey. The tectonic assembly consists of different units in varying ages, ranging from Paleozoic to Quaternary.

In the study and surrounding area, the geological units varying from old to young are Late Cretaceous-Paleocene-aged Caglayan and Bakirkoy Formations, and the Eocene aged Kaplica and Kabakoy Formations (Korkmaz and Gedik 1988; Guven 1993).

The oldest unit cropping out in the area is the Caglayan Formation, which is composed of basalt, andesite and pyroclastic rocks with intercalations of sandstone, marl and red limestone. This formation has a regionally significant lateral distribution. The Caglayan Formation is overlain by the Bakirkoy Formation which is composed of weathering of white-bordeaux colored marl, claystone and limestone. Further upwards, the Early-Middle Eocene aged Kaplica Formation which is composed of thick bedded and coarse sandstone, marl and intercalation of pyroclastic rocks follows

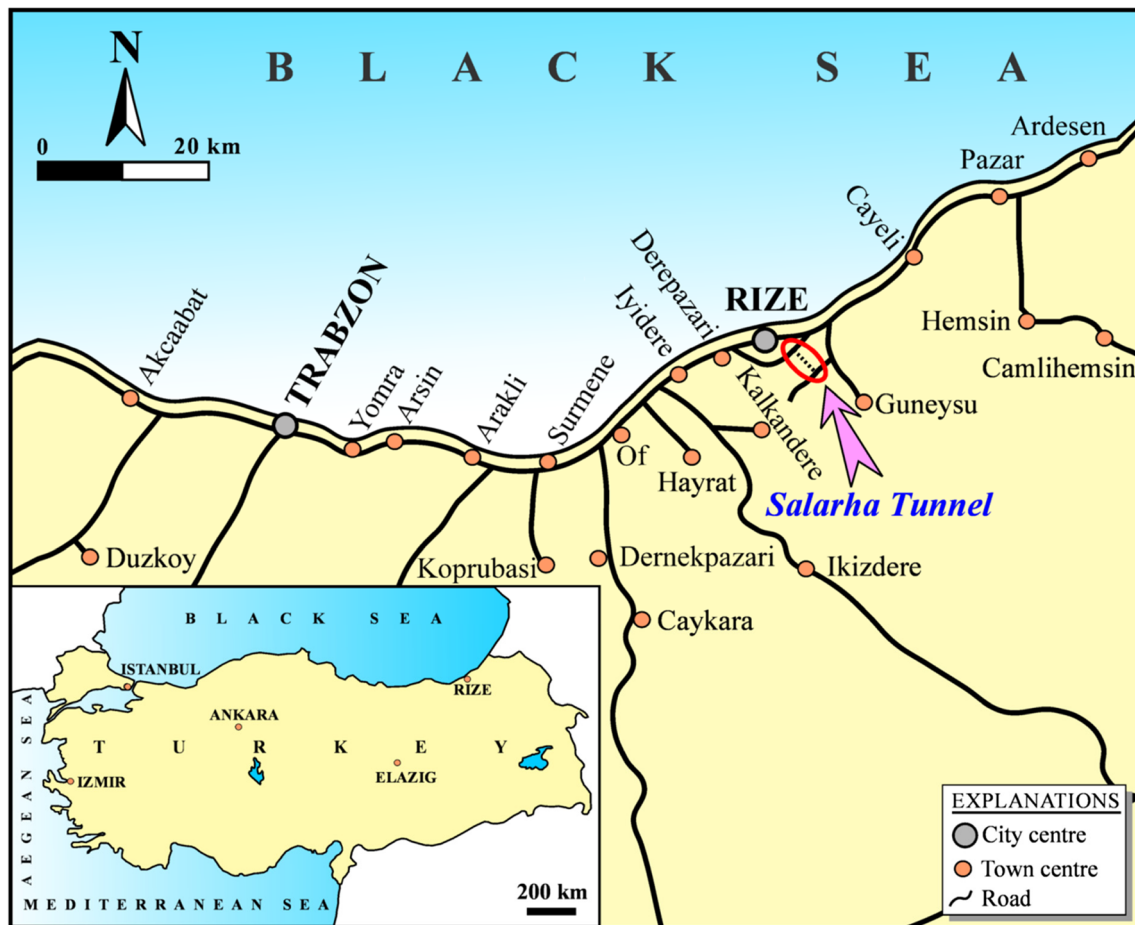


Fig. 1 Location map of the study area

the sequence by a slight unconformity. The Kaplica Formation passes upward into the Kabakoy Formation composing of andesite, basalt and agglomerates. The youngest unit in the area is the Quaternary-aged alluvium. A simplified geological map of the study and surrounding area is given in Fig. 2.

### Engineering geological investigations

Engineering geological properties of the rock masses cropping out along the Salarha Tunnel were determined by the help of field and laboratory studies. According to the geological cross-section along the tunnel alignment prepared by using the drilling and field study data, the tunnel ground was subdivided into five sections by considering their lithological, structural and geotechnical properties, and overburden. The geotechnical properties of the rock masses in the portal sections were also delineated. The five sections are shown in Fig. 3, illustrating the geological cross-section. The detailed information obtained from geotechnical studies are given in the following chapters.

### Field and laboratory studies

Field studies included geological mapping, scan-line survey and borehole investigations. Because of highly steep terrain and dense vegetation, nine investigation boreholes (Figs. 2 and 3) with a total length of 655 m were drilled by the KGM in order to observe the rock mass characteristics at the tunnel level, identify the discontinuity properties, assess the groundwater level and determine sampling for the laboratory tests. Two of the boreholes (BH 1–2) were located at the entrance portal, two boreholes (BH 8–9) at the exit portal in the tunnel section and another five (BH 3–7) towards the middle of the tunnel route.

Laboratory tests were performed on the core samples taken from the boreholes in accordance with the methods suggested by ISRM (2007) to determine the physico-mechanical properties of the rock materials including unit weight ( $\gamma$ ), uniaxial compressive strength ( $\sigma_{ci}$ ), Young's modulus ( $E_i$ ) and Poisson's ratio ( $\nu_i$ ). Furthermore, the rock quality designation (RQD) values were identified from the boreholes using the techniques suggested by Deere (1964). The quantitative description of the discontinuities in the rock masses such as

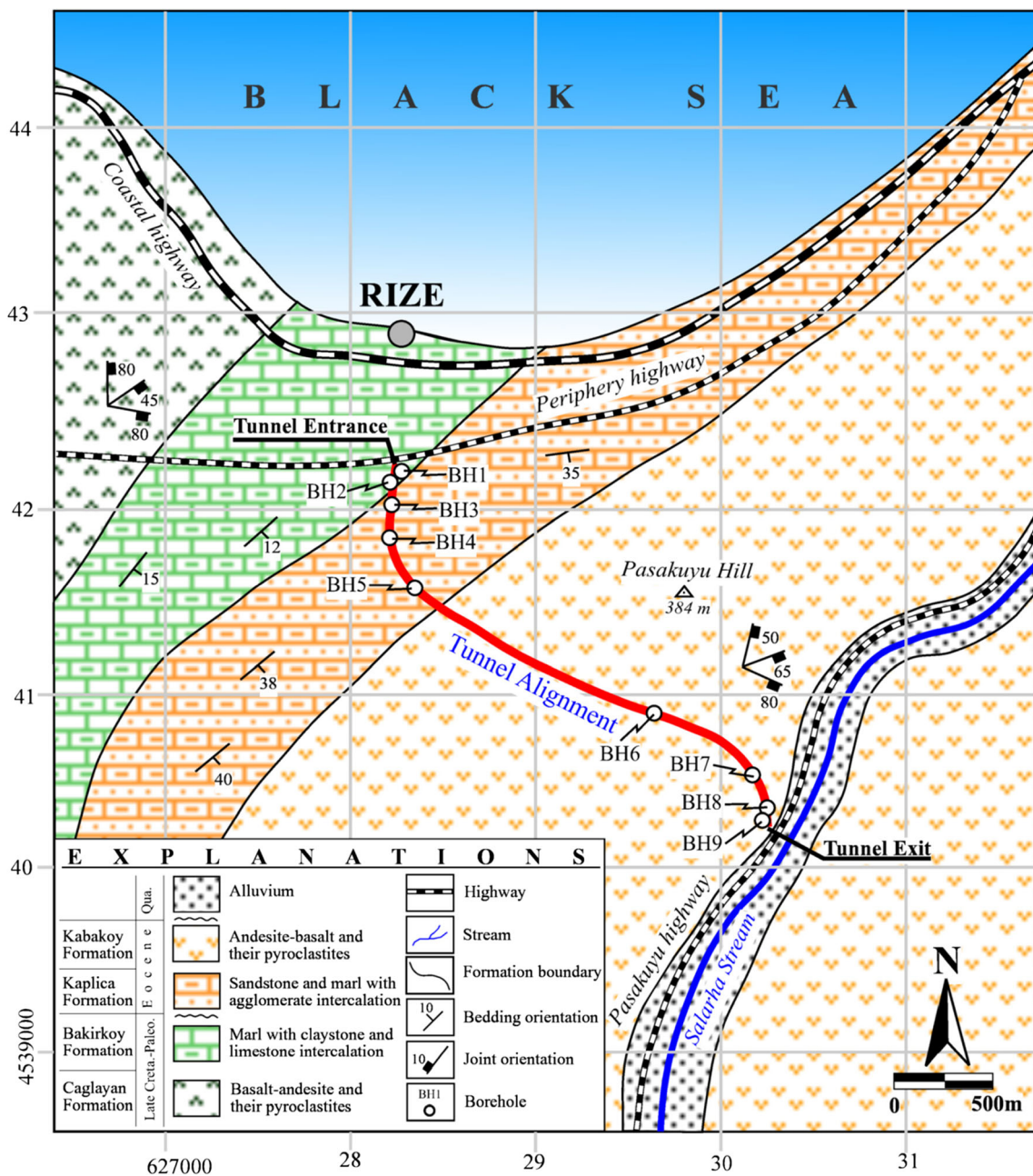


Fig. 2 Simplified geological map of the close vicinity of the study area (modified from Korkmaz and Gedik, 1988)

number of sets, spacing, persistence, infilling, roughness, aperture and weathering degree was defined by analyzing the cores and scan-line surveys according to the method suggested by ISRM (2007).

The entrance portal of the tunnel (section 1, ~7% of the tunnel) will be driven in the Bakirkoy Formation mainly consisting of marl and claystone. The uniaxial compressive strength value of the rock materials ranged from 6.06 to 70.47 MPa. The discontinuities in the rock masses are very closely spaced, with very high persistence, open (filled with soft clay and calcite), rough-planar and moderately to highly weathered. The RQD values range between 0 and 90%.

Approximately 25% of the tunnel (section 2) will be driven in sandstone, marl and agglomerate intercalation of the Kaplica Formation with strength values varying from 5.98 to 33.34 MPa. The discontinuities in the rock masses are closely spaced, with high persistence, open (filled with clay), rough-undulating and slightly to moderately weathered. The RQD ranges from 0 to 100%.

The rest of the tunnel (sections 3–5, approximately 68% of the tunnel) will be driven in the gray-colored agglomerates of the Kabakoy Formation. The strengths of the agglomerates ranged from 13.47 to 46.57 MPa. The discontinuities are commonly moderately spaced, with low persistence, open (filled

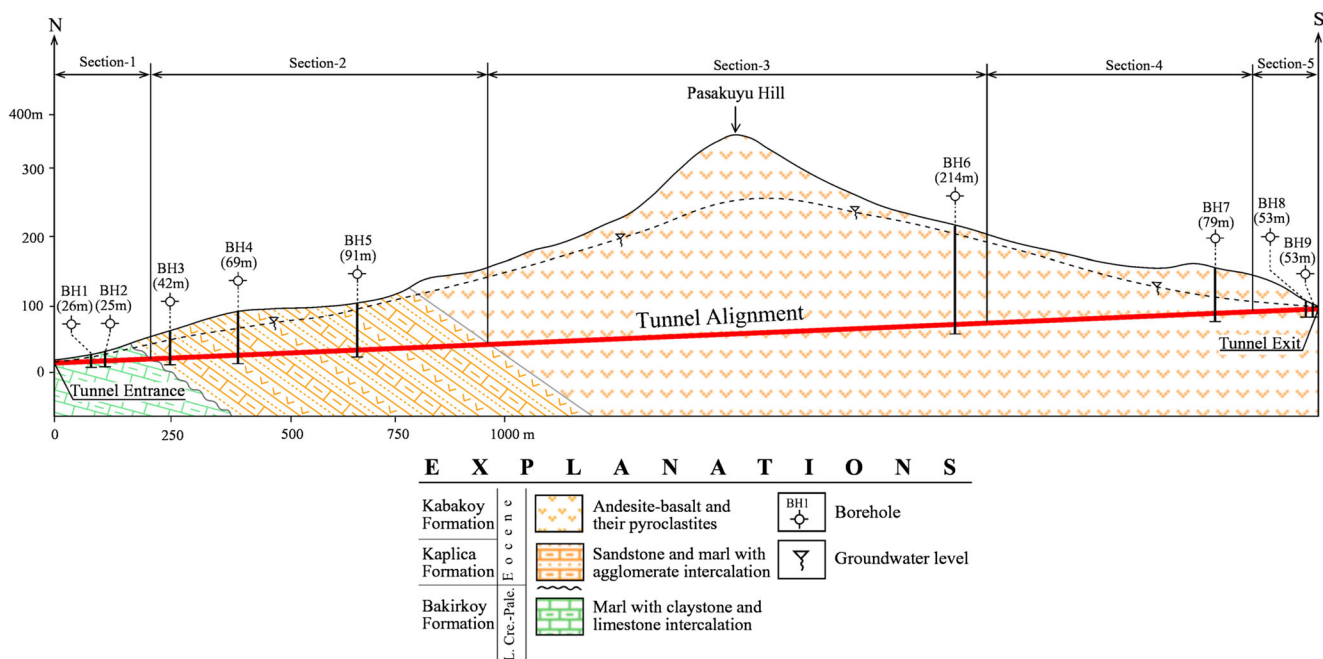


Fig. 3 Geological cross-section showing the borehole locations and sections along the tunnel alignment

with clay), rough-undulating and slightly to moderately weathered. The RQD value ranges between 0 and 100%.

Groundwater was reported at a depth ranging between 8.1 and 32.1 m. Although the discontinuities within the rock masses are generally closely spaced, low hydraulic conductivities are expected due to the filling of fractures with clays produced during weathering. These results show that the rock masses are generally dry and often show free water discharges such as leakages or drips.

Table 1 shows the laboratory test results and RQD values defined for five sections.

### Rock mass properties

The rock mass parameters such as Hoek–Brown constants ( $m_b$ ,  $s$  and  $a$ ), deformation modulus ( $E_m$ ), uniaxial compressive strength ( $\sigma_{cm}$ ), and Poisson’s ratio ( $\nu_m$ ) are necessary input parameters for the analytical and numerical analyses. In order to determine the rock mass parameters that utilize the geological strength index (GSI), the Hoek–Brown failure criterion proposed by Hoek et al. (2002) was used. The GSI value, Hoek–Brown constants,  $E_m$ ,  $\sigma_{cm}$  and  $\nu_m$  values were calculated using Eqs. 1–7 suggested by Hoek et al. (2013), Hoek et al. (2002),

Table 1 Physico-mechanical properties of the rock materials and RQD values

Properties	Section 1	Section 2	Section 3	Section 4	Section 5
Boreholes	BH1, BH2	BH3, BH4, BH5	BH6	BH7	BH8, BH9
Unit weight ( $\gamma$ , kN/m <sup>3</sup> )	(22.13–25.83) <sup>a</sup> 22.60	(21.62–27.68) <sup>a</sup> 24.94	(26.19–27.33) <sup>a</sup> 26.92	(23.29–27.56) <sup>a</sup> 25.37	(23.49–26.27) <sup>a</sup> 24.98
Uniaxial compressive strength ( $\sigma_{ci}$ , MPa)	(6.06–70.47) <sup>a</sup> 18.12	(5.98–33.34) <sup>a</sup> 30.10	(38.04–45.54) <sup>a</sup> 42.64	(15.53–28.41) <sup>a</sup> 20.31	(13.47–46.57) <sup>a</sup> 25.30
Young’s modulus ( $E_i$ , GPa)	(1.75–29.50) <sup>a</sup> 5.08	(1.67–19.95) <sup>a</sup> 8.56	(10.66–13.12) <sup>a</sup> 12.20	(3.54–8.07) <sup>a</sup> 5.79	(3.84–13.01) <sup>a</sup> 7.16
Poisson’s ratio ( $\nu_i$ )	(0.20–0.36) <sup>a</sup> 0.32	(0.19–0.36) <sup>a</sup> 0.27	(0.19–0.24) <sup>a</sup> 0.21	(0.22–0.22) <sup>a</sup> 0.29	(0.20–0.29) <sup>a</sup> 0.24
Rock quality designation (RQD, %)	(0–90) <sup>a</sup> 11	(0–100) <sup>a</sup> 57	(45–99) <sup>a</sup> 91	(30–100) <sup>a</sup> 80	(0–100) <sup>a</sup> 83

<sup>a</sup> Average value

**Table 2** Calculated rock mass parameters for the tunnel sections

Researcher	Equation	Note	Eq. no	Section 1	Section 2	Section 3	Section 4	Section 5
Hoek et al. (2013)	$GSI = 1.5JCond_{89} + RQD/2$		(1)	13	42	71	66	64
Hoek et al. (2002)	$m_b = m_i e^{\left(\frac{GSI-100}{28-14D}\right)}$		(2)	0.31	2.14	6.74	5.54	5.25
	$s = e^{\left(\frac{GSI-100}{9-3D}\right)}$		(3)	0.0001	0.0016	0.0399	0.0216	0.0183
	$a = \frac{1}{2} + \frac{1}{2} \left( e^{-GSI/15} - e^{-20/3} \right)$		(4)	0.570	0.510	0.501	0.502	0.502
	$\sigma_{cm} = \sigma_{ci} \cdot \frac{(m_b+4s-a(m_b-8s))(m_b/4+s)^{a-1}}{2(1+a)(2+a)}$	MPa	(5)	0.91	5.73	16.19	6.76	8.14
Hoek and Diederichs (2006)	$E_m = 100 \left( \frac{1-(D/2)}{1+e^{(75+25D-GSI)/11}} \right)$	GPa	(6)	0.17	1.57	9.16	3.72	4.37
Aydan et al. (1993)	$\nu_m = 0.25(1 + e^{-\sigma_{cm}/4})$		(7)	0.45	0.31	0.25	0.30	0.28
Cai et al. (2007)	$GSI_r = GSI e^{-0.0134GSI}$		(8)	11	24	27	27	27
	$m_{br} = m_i e^{\left(\frac{GSI_r-100}{28}\right)}$		(9)	0.29	1.12	1.42	1.41	1.41
	$s_r = e^{\left(\frac{GSI_r-100}{9}\right)}$		(10)	0.00005	0.00021	0.00031	0.00031	0.00031
	$a_r = \frac{1}{2} + \frac{1}{2} \left( e^{-GSI_r/15} - e^{-20/3} \right)$		(11)	0.580	0.534	0.527	0.527	0.527

$JCond_{89}$ : joint condition rating (Bieniawski 1989)

Hoek and Diederichs (2006), and Aydan et al. (1993), respectively.

Disturbance factor (D) was considered to be zero assuming the controlled blasting and mechanical excavation method was applied. The  $m_i$  constant of the rock materials was defined with the help of RocData v5.0 (Rocscience Inc. 2016a) software and taken as 7 for section 1, 17 for section 2 and 19 for sections 3–5.

In order to determine the post-peak behavior of the rock masses upon tunnel excavation, the method proposed by Cai et al. (2007) was applied. The residual GSI ( $GSI_r$ ) values and residual Hoek–Brown constants ( $m_{br}$ ,  $s_r$  and  $a_r$ ) were calculated using Eqs. 8–11.

The equations used in the calculations and estimated rock mass parameters are presented in Table 2.

### Rock mass classifications and empirical support design

In this study, most commonly utilized rock mass classification systems such as RMR, Q and NATM were employed to

characterize the rock masses along the tunnel alignment and to conduct empirical preliminary support design. In the classification systems, the data obtained from field studies, boreholes and laboratory tests were used.

The RMR system was proposed by Bieniawski (1974) and revised in 1989. The main input parameters of this system are the uniaxial compressive strength of the intact rock, RQD, discontinuity properties and groundwater conditions. In this study, the latest version of the RMR (Bieniawski 1989) system was considered. According to the RMR system, the quality of the rock masses along the Salarha Tunnel alignment varies from very poor to fair (Table 3).

The Q system was suggested by Barton et al. (1974) and it is also known as the Norwegian Technical Institute (NGI) system. This system is defined by the function of RQD,  $J_n$  (joint sets),  $J_r$  (joint roughness),  $J_a$  (joint alteration),  $J_w$  (water pressure) and stress reduction factor (SRF). The Q values of the rock masses were determined using the following equation:

**Table 3** RMR, Q and NATM classifications of the rock masses along the Salarha Tunnel

Section	Chainage (km)	Rock mass	Basic RMR	Adjusted RMR	Q	NATM
1	0 + 200–0 + 400	Bakirkoy Formation (entrance portal)	21.1	16.9/Very poor	0.03/Extremely poor	C1/Rock bursting
2	0 + 400–1 + 150	Kaplica Formation	35.2	33.1/Poor	0.32/Very poor	B3/Rolling
3	1 + 150–2 + 250	Kabakoy Formation (maximum overburden)	54.2	49.1/Fair	2.28/Poor	B2/Very friable
4	2 + 250–2 + 860	Kabakoy Formation	38.8	34.6/Poor	2.00/Poor	B2/Very friable
5	2 + 860–3 + 150	Kabakoy Formation (exit portal)	39.9	35.6/Poor	0.33/Very poor	B3/Rolling

$$Q = \left( \frac{RQD}{J_n} \right) \left( \frac{J_r}{J_a} \right) \left( \frac{J_w}{SRF} \right) \tag{12}$$

In terms of the Q values, the quality of the rock masses along the tunnel line ranges between extremely poor and very poor (Table 3).

The NATM system was developed by Ladislaus von Rabcewicz, Leopold Müller and Franz Pacher in Austria between 1957 and 1965. The main goal of the NATM is to use field stress of the surrounding rock mass in order to stabilize the underground opening itself (Bieniawski 1989). Considering the NATM-based Ö-NORM B2203 (1994) standard, the rock masses along the tunnel alignment were classified as rock bursting/C1, rolling/B3 and very friable/B2 (Table 3).

The empirical classification results show that the rock mass classification with the Q system lead to a more conservative classification than the RMR system for the geotechnical units. This difference might have resulted from different parameters which each classification system uses, and also their

sensitivity to the rock behaviors. Although both rock mass classification systems have been modified and improved continuously, the results vary with site conditions.

In rock tunnels, the RMR system suggests support elements only for the particular conditions (horseshoe-shaped span of 10 m, vertical stress lower than 25 MPa, drilling and blasting construction; Bieniawski, 1989). However, the excavation shape of the Salarha Tunnel is a modified horseshoe with a 12-m span. Therefore, the empirical preliminary support systems proposed by the Q system (Barton 2002) were applied for the Salarha Tunnel. Considering the empirical method, three support categories were determined (Table 4). The planned construction characteristics including construction phase, round length, stand-up time and support time are also presented in Table 4.

**Analytical tunnel support analyses**

In order to define the support requirements analytically, the convergence-confinement method was utilized. This

**Table 4** Empirical tunnel support categories for the rock masses along the Salarha Tunnel

Support type	B2/1 < Q < 4/Poor rock	B3/0.1 < Q < 0.4/Very poor rock	C1/0.01 < Q < 0.04/Extremely poor
Section	3 and 4	2 and 5	1
Construction phase	Top heading and bench	Top heading and bench	Top heading, bench and invert
Excavation method	Drill and blast	Drill and blast	Mechanical excavation
Round length	1.5–3.0-m advance in top heading and bench	1.0–1.5-m advance in top heading and bench	0.5–1.0-m advance in top heading, bench and invert
Stand-up time	~100 h	Immediate collapse	Immediate collapse
Support time	Commence support after each blast	Install support concurrently with excavation	Install support concurrently with excavation
Support requirements			
Roof	Systematic rock bolts 4 m long, spaced 1.7–2.1 m, and 50–90-mm-thick steel fiber/wire mesh-reinforced shotcrete (Sfr + B)	Systematic rock bolts 4 m long, spaced 1.3–1.5 m, and 120–150-mm-thick steel fiber/wire mesh-reinforced shotcrete (Sfr + B)	Systematic rock bolts 4 m long, spaced 1.0–1.2 m, and 150–250-mm-thick steel fiber/wire mesh-reinforced shotcrete (Sfr + B) and steel ribs (RRS)
Wall	Systematic rock bolts 3.5 m long, spaced 2.1–2.3 m, and 40–50-mm-thick steel fiber/wire mesh-reinforced shotcrete (Sfr + B)	Systematic rock bolts 3.5 m long, spaced 1.5–1.7 m, and 90–120-mm-thick steel fiber/wire mesh-reinforced shotcrete (Sfr + B)	Systematic rock bolts 3.5 m long, spaced 1.0–1.2 m, and 150–250-mm-thick steel fiber/wire mesh-reinforced shotcrete (Sfr + B) and steel ribs (RRS)
Invert	–	–	Systematic rock bolts 3.5 m long, spaced 1.0–1.2 m, and 150–250-mm-thick steel fiber/wire mesh-reinforced shotcrete (Sfr + B) and steel ribs (RRS)

methodology has been described by Carranza-Torres and Fairhurst (1999) for rock masses that satisfy the Hoek–Brown criterion. Convergence-confinement is a procedure that allows the load imposed on a support installed behind the face of tunnel to be estimated. Application of the method requires knowledge of the deformation characteristics of the ground and of the support (Basarir 2006). In this method, a tunnel of radius  $R$  subjected to far-field stress  $\sigma_o$  and uniform internal pressure  $p_i$  is considered. The scaled internal pressure  $P_i$  and scaled far-field stress  $S_o$  are defined as (Carranza-Torres and Fairhurst 2000);

$$P_i = \frac{p_i}{m_b \sigma_{ci}} + \frac{s}{m_b^2} \tag{13}$$

$$S_o = \frac{\sigma_o}{m_b \sigma_{ci}} + \frac{s}{m_b^2} \tag{14}$$

where  $m_b$  and  $s$  are the Hoek–Brown constants,  $\sigma_{ci}$  is the uniaxial compressive strength of intact rock (MPa),  $p_i$  is the uniform internal (support) pressure (MPa) and  $\sigma_o$  is the far-field stress (MPa).

The scaled critical internal pressure  $P_i^{cr}$  for which the elastic limit is achieved is defined as (Carranza-Torres and Fairhurst 2000);

$$P_i^{cr} = \frac{1}{16} \left[ 1 - \sqrt{1 + 16S_o} \right]^2 \tag{15}$$

The actual critical internal pressure  $p_i^{cr}$  is found from the inverse of Eq. (13);

$$p_i^{cr} = \left[ P_i^{cr} - \frac{s}{m_b^2} \right] m_b \sigma_{ci} \tag{16}$$

If the uniform internal pressure  $p_i$  is greater than this actual critical internal pressure  $p_i^{cr}$ , no failure will occur. In this case, the behavior of surrounding rock mass is elastic and the inward elastic displacement of tunnel wall  $u_r^{el}$  is given by:

$$u_r^{el} = \frac{\sigma_{ci} - P_i}{2G_m} R \tag{17}$$

where  $G_m$  is the shear modulus of rock mass (GPa) and  $R$  is the radius of tunnel (m).

If the uniform internal pressure  $p_i$ , on the other hand, is less than the actual critical internal pressure  $p_i^{cr}$ , failure is expected to occur. Then, the radius of the broken zone  $R_{pl}$  is defined by:

$$R_{pl} = R \exp \left[ 2 \left( \sqrt{P_i^{cr}} - \sqrt{P_i} \right) \right] \tag{18}$$

Hoek and Brown (1997) suggested the following equation to evaluate the total plastic deformation  $u_r^{pl}$  for rock masses:

$$\begin{aligned} \frac{u_r^{pl}}{R} \frac{2G_m}{\sigma_o - P_i^{cr}} = & \left[ \frac{1 - 2\nu_m}{2} \frac{\sqrt{P_i^{cr}}}{S_o - P_i^{cr}} + 1 \right] \left( \frac{R_{pl}}{R} \right)^2 \\ & + \left[ \frac{1 - 2\nu_m}{4(S_o - P_i^{cr})} \right] \left[ \ln \left( \frac{R_{pl}}{R} \right) \right]^2 - \left[ \frac{1 - 2\nu_m}{2} \frac{\sqrt{P_i^{cr}}}{S_o - P_i^{cr}} \right] \\ & \left[ 2 \ln \left( \frac{R_{pl}}{R} \right) + 1 \right] \end{aligned} \tag{19}$$

The vertical stress ( $\sigma_v$ ) is assumed as an increasing trend with depth owing to its overburden weight. The loading condition for vertical stresses was determined by:

$$\sigma_v = \gamma H \tag{20}$$

where  $\gamma$  is the unit weight of rock mass (MN/m<sup>3</sup>) and  $H$  is the overburden depth (m).

It is known that the undisturbed horizontal stress ( $\sigma_h$ ) is a variable at shallow depth and tends to a hydrostatic state in deep medium (Hoek and Brown 1978). The horizontal stress was estimated from the following equation suggested by Sheorey et al. (2001):

$$\sigma_h = \frac{\nu_m}{1 - \nu_m} \sigma_v + \frac{\beta E_m G}{1 - \nu_m} (H + 1000) \tag{21}$$

where  $\beta$  is the coefficient of linear thermal expansion ( $8 \times 10^{-6}/^\circ\text{C}$ ),  $G$  is the geothermal gradient ( $0.024 \text{ }^\circ\text{C/m}$ ),  $\nu_m$  is the Poisson’s ratio of rock mass and  $E_m$  is the deformation modulus of rock mass (GPa).

The far-field stress  $\sigma_o$  was calculated using the following equation (Carranza-Torres and Diederichs 2009):

$$\sigma_o = \frac{\sigma_v + \sigma_h}{2} \tag{22}$$

Carranza-Torres and Fairhurst (2000) suggested the following equation for calculating rock mass shear modulus:

$$G_m = \frac{E_m}{2(1 + \nu_m)} \tag{23}$$

Noncircular tunnel cross-sections are common in practice, but the convergence-confinement method assumes circular tunnel shapes. In order to calculate the deformations and radius of the failure zone, Curran et al. (2003) proposed approximation of the noncircular cross-section with an equivalent circular tunnel of the same cross-sectional area. The equivalent diameter  $D$  was calculated using the following



relationship and half of this value was taken as the tunnel radius in calculations:

$$D = \sqrt{\frac{4A}{\pi}} \tag{24}$$

where A is the area of tunnel cross-section in m<sup>2</sup> (in this study, the A value was taken as 99 m<sup>2</sup> for section 1 and as 91 m<sup>2</sup> for sections 2–5).

In this study, the analytical analyses were performed in two steps. In the first step, the uniform internal pressure p<sub>i</sub> was assumed to be zero for the unsupported tunnel case. The necessary rock properties were changed according to the formation and they were used as input. The calculated parameters of each tunnel section are summarized in Table 5.

Apart from section 5, the plastic zones were developed around the tunnel. The maximum deformations for the unsupported tunnel in sections 1–5 were found to be 2.35, 0.78,

0.39, 0.45 and 0.48 cm, respectively. The maximum total displacement value for section 1 is much higher than all the other sections. However, the average total displacement values for the tunnel are very small. Strain is defined as percentage of the ratio of tunnel closure to tunnel radius. In the present study, the strain values for sections 1–5 were calculated as 0.42, 0.15, 0.07, 0.08 and 0.09%, respectively, as shown in Table 5. Hoek and Marinos (2000) suggested that for formations with strain values less than 1%, few stability problems are expected. Therefore, the application of the support systems proposed by empirical analysis is recommended.

In the second step, the maximum pressure p<sub>s</sub><sup>max</sup> and the elastic stiffness K<sub>s</sub> of the suggested support systems were determined for each section. The extent of the failure zone and the amount of deformation in the rock mass surrounding the tunnel can be controlled by the application of an internal support pressure. This support can be provided by combinations of shotcrete, rock bolts and steel sets. Hoek (2007) and Carranza-Torres and Engen (2017) suggested equations calculating the capacity of

**Table 5** Results of the convergence-confinement analyses for the Salarha Tunnel

	Section 1	Section 2	Section 3	Section 4	Section 5
Uniform internal pressure, p <sub>i</sub> (MPa)	0	0	0	0	0
Vertical stress, σ <sub>v</sub> (MPa)	0.45	2.24	7.81	3.30	1.50
Horizontal stress, σ <sub>h</sub> (MPa)	0.37	1.01	2.67	1.39	0.59
Far-field stress, σ <sub>o</sub> (MPa)	0.41	1.63	5.24	2.34	1.05
Scaled far-field stress, S <sub>o</sub> (MPa)	0.07	0.03	0.02	0.02	0.01
Shear modulus, G <sub>m</sub> (GPa)	0.06	0.60	3.65	1.43	1.70
Equivalent diameter, D (m)	11.22	10.76	10.76	10.76	10.76
Equivalent radius, R (m)	5.61	5.38	5.38	5.38	5.38
Scaled critical internal pressure, P <sub>i</sub> <sup>cr</sup> (MPa)	0.01394	0.00219	0.00127	0.00159	0.00027
Actual critical internal pressure, p <sub>i</sub> <sup>cr</sup> (MPa)	0.075	0.119	0.113	0.100	−0.052
Elastic displacement, u <sub>r</sub> <sup>el</sup> (mm)	0.00	0.00	0.00	0.00	4.79
Plastic displacement, u <sub>r</sub> <sup>pl</sup> (mm)	23.55	7.80	3.88	4.47	0.00
Equivalent radius of the failure zone, R <sub>pl</sub> (m)	6.76	5.69	5.45	5.53	0.00
Strain, ε (%)	0.42	0.15	0.07	0.08	0.09
Maximum support pressure provided by shotcrete, p <sub>sc</sub> <sup>max</sup> (MPa)	0.87	0.55	0.33	0.33	0.55
Elastic stiffness of shotcrete, K <sub>sc</sub> (MPa/m)	0.17	0.11	0.07	0.07	0.11
Maximum support pressure provided by rock bolt, p <sub>sb</sub> <sup>max</sup> (MPa)	0.25	0.15	0.09	0.09	0.15
Elastic stiffness of rock bolt, K <sub>sb</sub> <sup>max</sup> (MPa/m)	0.03	0.02	0.01	0.01	0.02
Maximum support pressure provided by steel set, p <sub>ss</sub> <sup>max</sup> (MPa)	0.39	–	–	–	–
Elastic stiffness of steel set, K <sub>ss</sub> (MPa/m)	34.43	–	–	–	–
Maximum support pressure provided by combined support, p <sub>s</sub> <sup>max</sup> (MPa)	0.39	0.64	0.39	0.39	0.64
Elastic stiffness of combined support, K <sub>s</sub> (MPa/m)	34.63	0.13	0.08	0.08	0.13
Maximum elastic deformation of the combined support, u <sub>r</sub> <sup>max</sup> (m)	0.01	5.02	5.08	5.08	5.02

shotcrete, rock bolts and steel sets for a tunnel in a hydrostatic stress field.

The maximum support pressure provided by shotcrete and the elastic stiffness of shotcrete were estimated from the following equations:

$$p_{sc}^{\max} = \frac{\sigma_c}{2} \left[ 1 - \frac{(r_o - t_c)^2}{r_o^2} \right] \quad (25)$$

$$K_{sc} = \frac{E_c (r_o^2 - (r_o - t_c)^2)}{2(1 - \nu_c^2)(r_o - t_c)r_o^2} \quad (26)$$

where  $\sigma_c$  is the uniaxial compressive strength of the shotcrete (MPa),  $E_c$  is the Young's modulus of the shotcrete (MPa),  $\nu_c$  is the Poisson's ratio of the shotcrete,  $t_c$  is the thickness of the shotcrete (m) and  $r_o$  is the radius of the tunnel (m).

The maximum support pressure provided by the rock bolts system and the elastic stiffness of rock bolts were determined from the given equations:

$$p_{sb}^{\max} = \frac{T_{bf}}{s_l s_c} \quad (27)$$

$$K_{sb} = \frac{E_b \pi d_b^2}{4l s_l s_c} \quad (28)$$

where  $T_{bf}$  is the ultimate bolt load obtained from a pull-out test (MN),  $E_b$  is the Young's modulus of the rock bolt (MPa),  $d_b$  is the rock bolt diameter (m),  $l$  is the free length of the bolt (m),  $s_c$  is the circumferential bolt spacing (m) and  $s_l$  is the longitudinal bolt spacing (m).

The maximum support pressure of steel sets in direct contact with the rock and the elastic stiffness of steel sets were calculated from the following equations:

$$p_{ss}^{\max} = \frac{A_s \sigma_s}{s_l r_o} \quad (29)$$

$$K_{ss} = \frac{E_s A_s}{s_l r_o^2} \quad (30)$$

where  $\sigma_s$  is the yield strength of the steel (MPa),  $E_s$  is the Young's modulus of the steel (MPa),  $A_s$  is the cross-sectional area of the section (m<sup>2</sup>),  $s_l$  is the set spacing along the tunnel axis (m) and  $r_o$  is the radius of the tunnel (m).

If more than one of the support systems described earlier is installed at the same location, their combined effect can be determined by adding the stiffnesses for each of the individual supports. The stiffness  $K_s$  for the three systems acting together was computed as:

$$K_s = K_{sc} + K_{sb} + K_{ss} \quad (31)$$

The  $K_s$  value was assumed to remain valid until one of the three supports achieves its maximum possible elastic deformation, and it was computed using the following equation:

$$u_r^{\max} = \frac{p_s^{\max}}{K_s} \quad (32)$$

where  $u_r^{\max}$  is the maximum possible elastic deformation of the combined support system (m).

In the convergence-confinement method, the combined support system is assumed to fail at that point. The support with the lowest value of  $u_r^{\max}$  determines the maximum support pressure available for the three supports acting together. The support patterns and characteristics of the shotcrete, rock bolt and steel set were same as those proposed in Table 4 and Table 7. The maximum support pressure values for each section were calculated as 0.39, 0.64, 0.39, 0.39 and 0.64 MPa, respectively (Table 5). According to obtained results, the maximum support pressure values are higher than the actual critical internal (support) pressure values. Therefore, the suggested empirical support design is satisfactory for the tunnel stability.

## 2D and 3D numerical tunnel support analyses

The use of the 3D numerical models in underground excavations requires expensive software and great computational hardware and they are time-consuming procedures. Because of these limitations, most of the above-mentioned researchers usually prefer to use 2D modeling software. However, the results of 2D analyses are often less satisfactory in terms of deformation and strain estimations when compared to the results of the analytical analyses. Therefore, it is of major importance to test the validity and performance of the numerical models developed in 2D plane strain models. In this respect, the 3D numerical models are useful tools that allow designers to compare and control the validity of 2D analysis results.

In this study, to determine the deformations and failure zones around the tunnel excavation and to verify the results of the empirical and analytical methods, the FEM-based 2D software RS<sup>2</sup> v9.0 and 3D software RS<sup>3</sup> v1.0 developed by Rocscience (2017, 2016b) were used in the numerical analyses. An automatic mesh around the tunnel was generated and

based on the elasto-plastic analysis, stresses and deformations were computed in these programs. In order to analyze the deformations and tunnel stability, and to explore the concept of rock support interaction, a simple model was used. Six-noded triangular finite elements were chosen in the mesh and finer zoning was applied around the excavation. Based on the construction procedure of the NATM (KGM 2013), the excavation boundary of the tunnel was generated considering its width and height in three stages as top heading, bench and invert for section 1 (Fig. 4a) and top heading and bench for the other sections (Fig. 4b). The outer model boundary was set to be at a distance of 10 times the radius of the tunnel. To simulate the tunnel excavation in all rock masses, five finite element models were generated using the same tunnel geometry, mesh and different material properties. The slice thickness was chosen as 10 m in the 3D analyze models. A Hoek–Brown failure criterion was used to determine the plastic zones in the vicinity of tunnel. Because the active North Anatolian Fault (NAF), which is the main source of the earthquake hazard in the Black Sea region, is located approximately 170 km south of the Salarha Tunnel, the analyses were performed only for the static conditions. The rock mass parameters used in the numerical analyses are presented in Table 6.

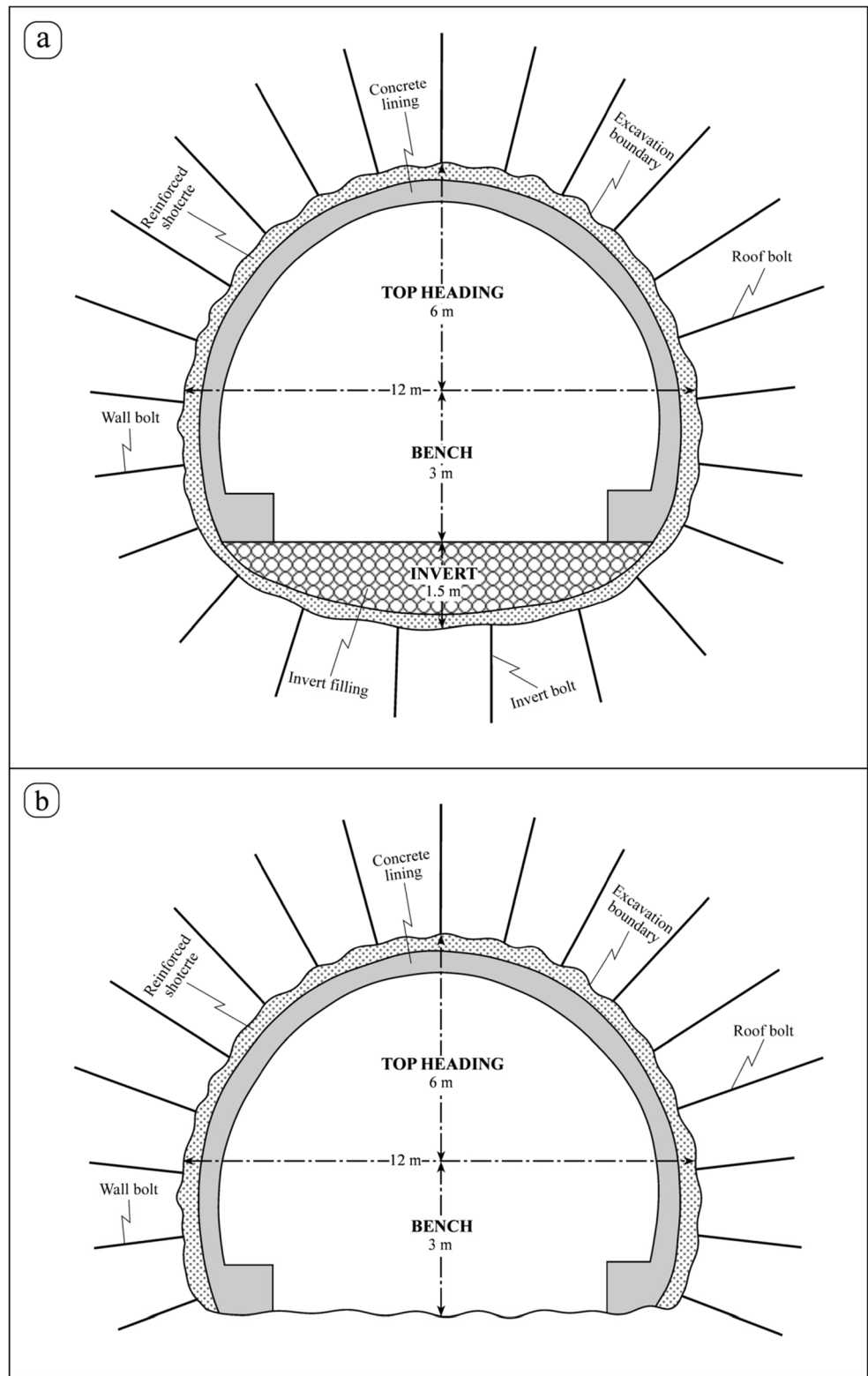
The numerical analyses were performed in two steps as unsupported and supported cases for each tunnel section. In the first step, following the examination of the maximum total displacements developed around the tunnel excavations without any support (Figs. 5 and 6), the maximum thicknesses of the plastic zone was determined. The maximum total displacement values around the tunnel show the progression of displacement on the excavation boundary before the support installation. According to the 2D analyses, the maximum total displacement values for all sections vary between 0.28–3.65 cm (Fig. 7). However, when considering the 3D analyses, the maximum total displacement values are very small and vary between 0.21–2.00 cm (Fig. 7). Furthermore, there is a difference between the deformation mechanism of the 2D and 3D models for section 5. Considering the 2D model, an exaggerated deformation has occurred at the outer walls. On the other hand, according to the 3D model, a limited deformation was observed at the tunnel walls (Fig. 6). This is an interesting find and an unexpected result of the 2D analysis, because small displacements at the excavation walls are expected under low in-situ stresses. In general, the total displacement concentrations in the 2D models are greater than that of the 3D models. The reason in these differences may be that in the 2D model, the excavation perpendicular to the paper is infinitive. Meanwhile, in the same direction, the excavation dimension is only 10 m in the 3D model. Moreover, similar results with the 3D FEM analyses have been obtained by the convergence–confinement analyses and the maximum total displacement values vary between 0.39–2.35 cm (Fig. 7). The analytical

method used in the paper seems to be in a relatively good agreement with the 3D finite element computational results, and proves that the use of 3D modeling in design of the underground excavation seems to be reliable.

It can be seen from Fig. 7 that the maximum total displacement value for section 1 is much higher than all the other sections. The overall total displacement values for the tunnel are very small. However, the extent of the plastic zones shows that there would be a stability problem in section 1; a few block falls in sections 2–5, if they are not supported. The plastic zones developed around the unsupported tunnel boundary are illustrated in Figs. 8 and 9. It should be remembered that RS<sup>2</sup> and RS<sup>3</sup> are small-strain FEM-based programs and, therefore, it cannot accommodate the very large strains. Therefore, it is more important to consider the extent of the plastic zone rather than the magnitude of the displacements. When Figs. 8 and 9 are examined, the most problematic section along the tunnel route is section 1 driven in the Bakirkoy Formation. Maximum total displacement and a larger plastic zone were developed in this section. Except for sections 1 and 5, the maximum plastic zone concentrations developed at the top of the excavations depending on the increased in situ stresses (Figs. 8 and 9). According to the 2D models, the extents of the plastic zone for the sections are 4.39, 1.67, 2.14, 2.15 and 0.00 m, respectively. On the other hand, the plastic zones in the 3D models could not be measured, since the RS<sup>3</sup> v1.0 software does not have a ruler option. However, when the plastic zones developed around the unsupported tunnel excavation, presented in Figs. 8 and 9, are compared, it is clearly seen that the extent of the plastic zones in the 3D models are relatively greater than that of the 2D analysis, especially in sections 2, 4 and 5. Unlike the 3D analyses, the results obtained from the 2D numerical modeling (0.00–4.39 m) are smaller than the convergence–confinement method (0.00–6.76 m). This is mainly due to the lost arching action in the 2D models. It is also thought that these differences are caused by a finite discretization in the numerical model.

In the second step, the performance of the empirical preliminary support design obtained from the Q classification system was investigated using the same unsupported 2D and 3D analysis models. The support patterns such as bolt length and spacing, and thickness of shotcrete were same as those proposed in Table 4, and their characteristics applied in numerical analyses are presented in Table 7. Changes in the maximum total displacements and extent of the plastic zones after support applications were analyzed and results were compared with the unsupported cases. Considering the 2D and 3D analyses results, the maximum total displacement values for all supported sections vary between 0.26–1.56 cm and 0.15–0.57 cm, respectively. After support installation, the magnitude of the displacements was slightly reduced except in section 1 (Fig. 7). Compared to the 3D models, it was observed

**Fig. 4** Tunnel excavation sections for the Salarha Tunnel



that no wall and crown deformations developed in the 2D models of sections 3 and 4 (Fig. 6). However, in the 2D models of sections 2 and 5, an exaggerated displacement concentration indicating a failure occurred at the outer

walls. Unlike the 2D analysis results, the acceptable total displacements in the 3D models of all sections took place inside the supported zone and these results confirm the tunnel stability (Figs. 5 and 6).

**Table 6** Material properties of the rock masses for the 2D and 3D numerical analyses

	Section 1	Section 2	Section 3	Section 4	Section 5
Elastic type	Isotropic	Isotropic	Isotropic	Isotropic	Isotropic
Rock mass strength, $\sigma_{cm}$ (MPa)	0.91	5.73	16.19	6.76	8.14
Deformation modulus, $E_m$ (GPa)	0.17	1.57	9.16	3.72	4.37
Poisson's ratio, $\nu_m$	0.45	0.31	0.25	0.30	0.28
Material type	Plastic	Plastic	Plastic	Plastic	Plastic
$m_i$ constant	7	17	19	19	19
$m_b$ constant	0.31	2.14	6.74	5.54	5.25
$s$ constant	0.0001	0.0016	0.0399	0.0216	0.0183
$a$ constant	0.570	0.510	0.501	0.502	0.502
$m_{br}$ residual constant	0.29	1.12	1.42	1.41	1.41
$s_r$ residual constant	0.00005	0.00021	0.00031	0.00031	0.00031
$a_r$ residual constant	0.580	0.534	0.527	0.527	0.527
Disturbance factor (D)	0	0	0	0	0
Dilation parameter	0	0	0	0	0
Vertical stress, $\sigma_v$ (MPa)	0.45	2.24	7.81	3.30	1.50
Horizontal stress, $\sigma_h$ (MPa)	0.37	1.01	2.67	1.39	0.59

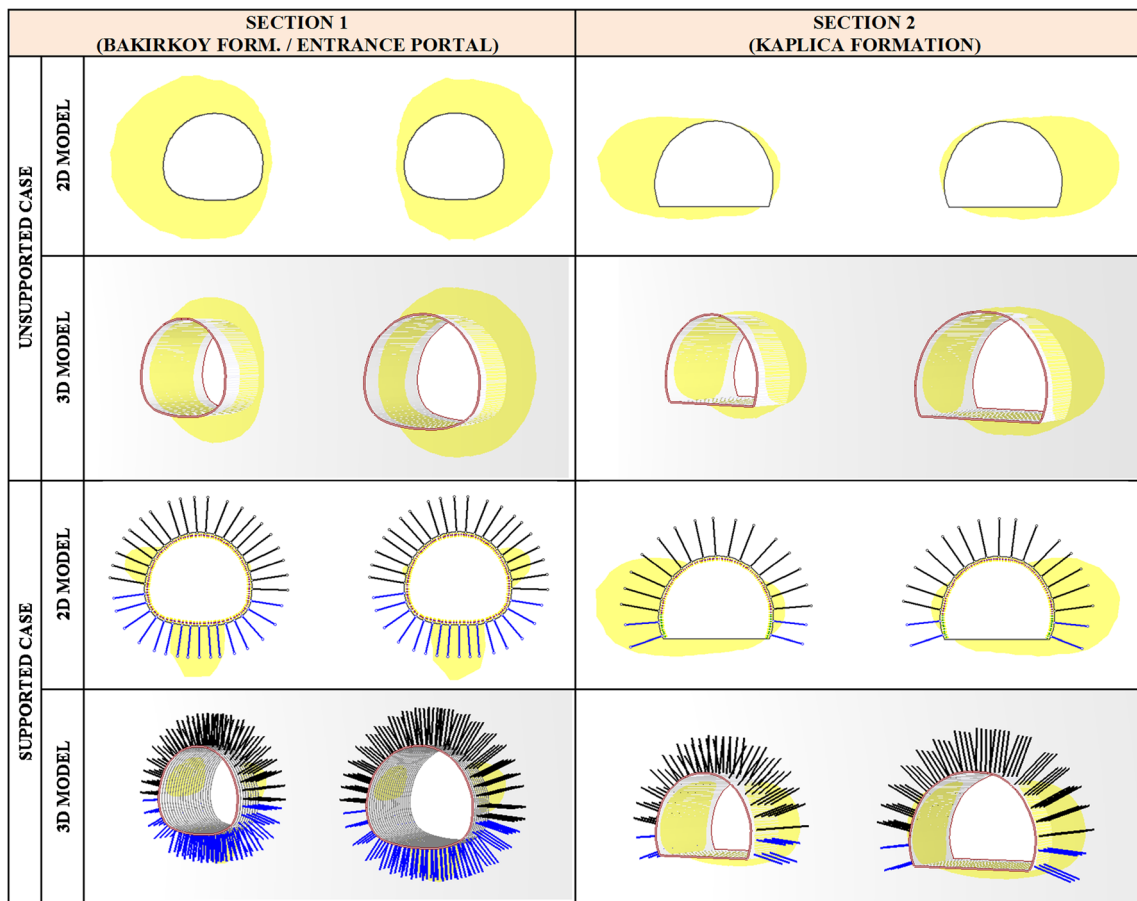


**Fig. 5** The graph showing the maximum total displacement variations along the tunnel line for the unsupported and supported cases according to 2D and 3D numerical analyses

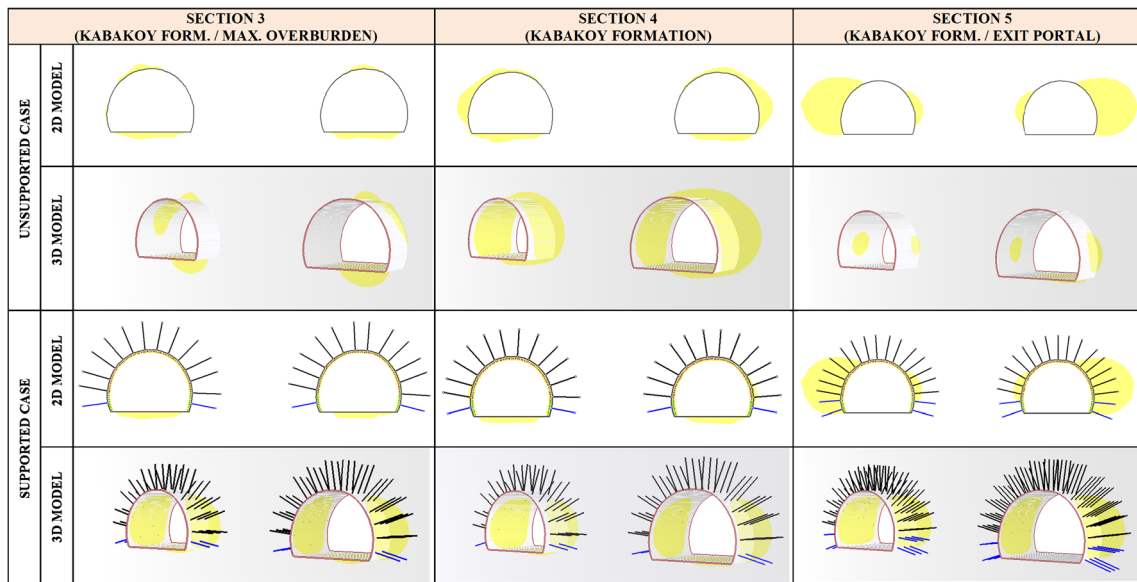
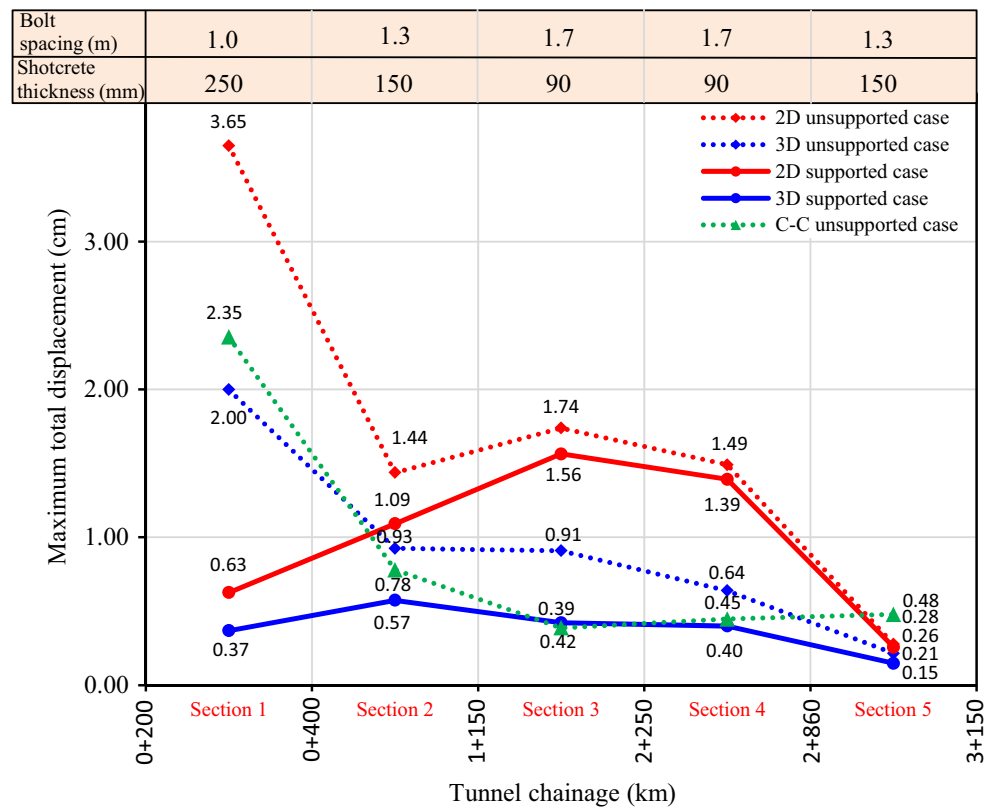


**Fig. 6** 2D and 3D numerical analyses showing the maximum total displacement developed in the sections 1 and 2 for the unsupported and supported cases

Moreover, compared to unsupported cases, the extent of the plastic zones has been reduced significantly by application of the shotcrete and rock bolts for all sections (Figs. 8 and 9). After the support application, the extent of the failure zone observed in the 2D models of all sections decreased from

0.00–4.39 m to 0.00–2.21 m. On the other hand, as can be seen from the 3D models given in Figs. 8 and 9, the plastic zones have hardly ever occurred. The empirical support applications have been effective in reducing failure around the most problematic section 1 driven in the Bakirkoy Formation

**Fig. 7** 2D and 3D numerical analyses showing the maximum total displacement developed in the sections 3, 4 and 5 for the unsupported and supported cases



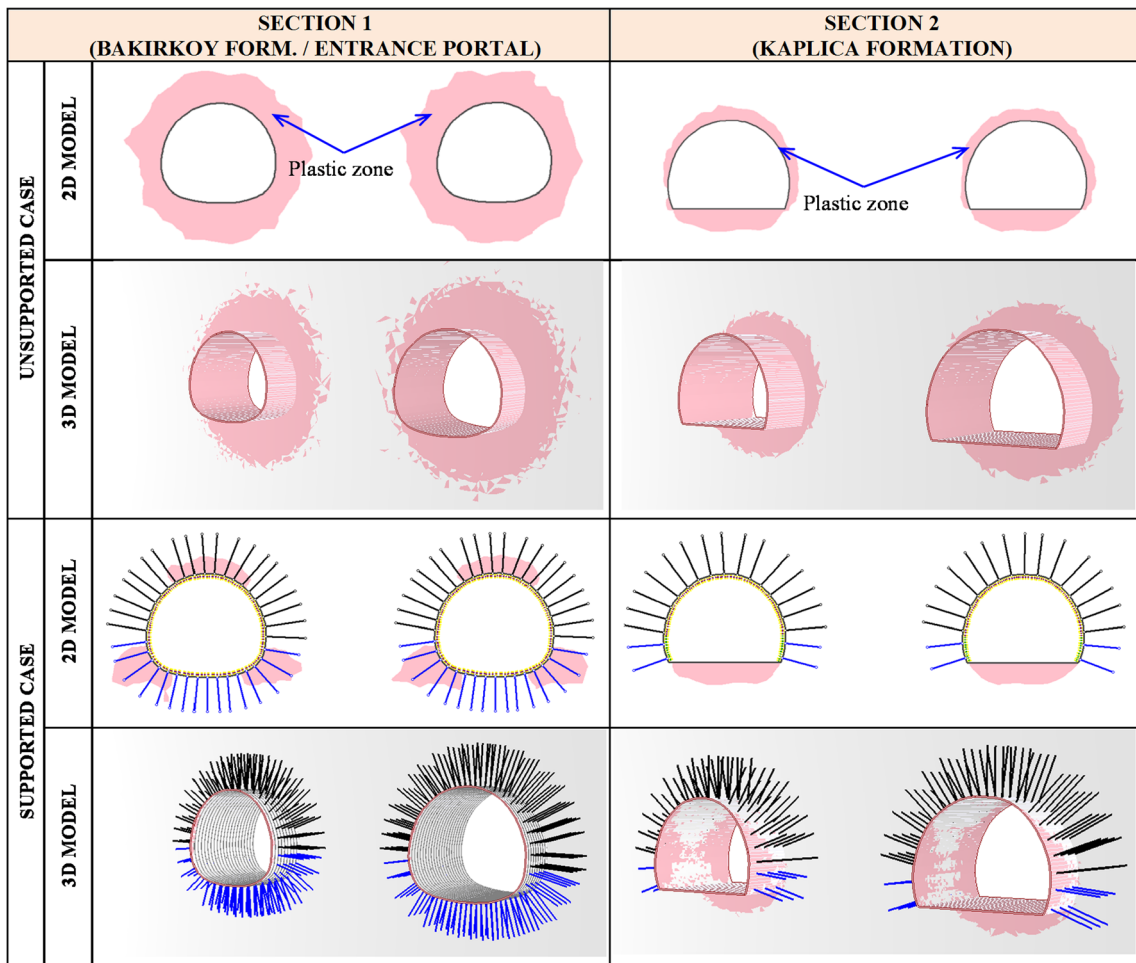


Fig. 8 2D and 3D numerical analyses showing the plastic zones developed in sections 1 and 2 for the unsupported and supported cases

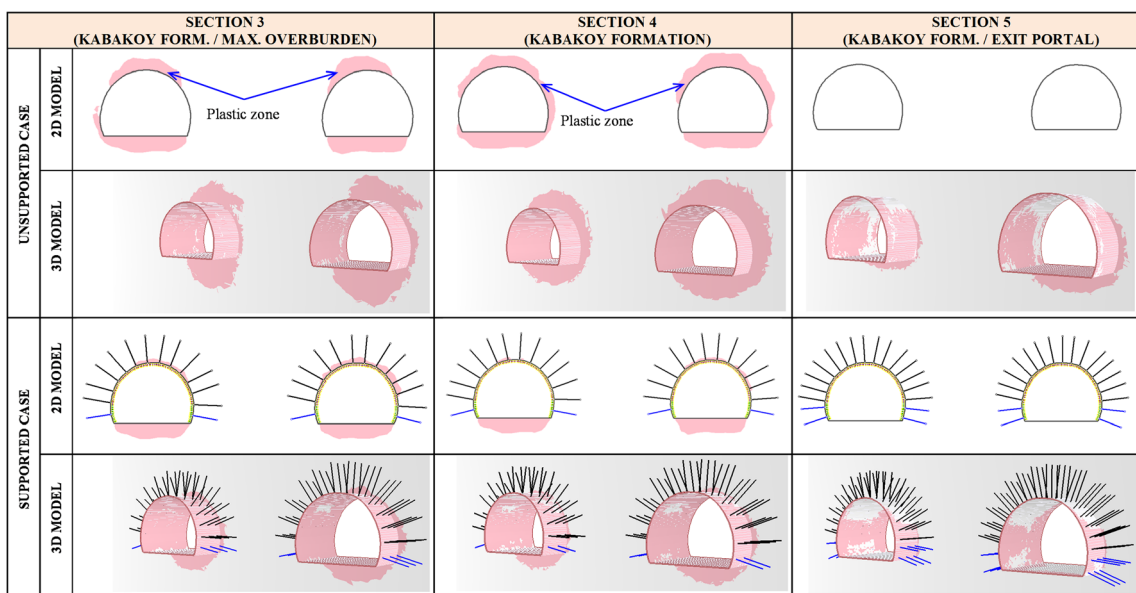


Fig. 9 2D and 3D numerical analyses showing the plastic zones developed in sections 3, 4 and 5 for the unsupported and supported cases

**Table 7** The characteristics of the support units used in the numerical analyses (KGM 2013)

Properties	Shotcrete	Wire mesh	Rock bolt	Steel set
Young's modulus ( $E$ , GPa)	20	200	200	200
Poisson's ratio ( $\nu$ )	0.2	0.35	–	0.35
Peak uniaxial compressive strength ( $\sigma_{cp}$ , MPa)	20	400	–	400
Residual uniaxial compressive strength ( $\sigma_{cr}$ , MPa)	3.5	–	–	–
Peak tensile strength ( $\sigma_{tp}$ , MPa)	3.1	500	–	500
Residual tensile strength ( $\sigma_{tr}$ , MPa)	0	–	–	–
Peak load (MN)	–	–	0.25	–
Residual load (MN)	–	–	0.025	–
Type	–	Ø6.5 mm, 150 × 150 mm	Ø28 mm fully bonded	I-beam 160 cm × 17.9 kg/m

(Fig. 8). The heaviest support elements, including steel sets, were applied to the extremely poor rock mass quality section 1. According to 2D analysis results of section 1, there are still plastic zones at the level of the invert and crown, unlike in the 3D model (Fig. 8). It was observed that the plastic zones in the 3D models are inside the region of the installed rock bolt support for all sections (Figs. 8 and 9). As a result, both convergence-confinement and 3D analyses proved that the empirical support design suggested by the Q system was sufficient to eliminate the stability problems in the tunnels.

Finally, the results of the convergence-confinement method in all issues related to the deformational aspects and performance of the empirical support design were in better agreement with the corresponding results of the 3D FEM analyses. The 3D FEM analyses may be very useful for the tunnel engineers in order to determine the tunnel safety in a more accurate way as compared to the 2D FEM analyses method. 3D finite element analysis gives a more realistic solution of rock-support interaction and the availability of modern geotechnical engineering software has facilitated the work.

## Conclusions

In this study, the preliminary support design of the Salarha Tunnel, which is planned to be constructed in Rize City, Turkey, was investigated. Based on the collected data from field and laboratory studies, the rock mass along the tunnel was characterized by means of the RMR, Q and NATM classification systems. After the application of the rock mass classifications, the three preliminary support categories and the related geotechnical rock mass parameters forming the tunnel were determined. In order to define the support requirements analytically, the convergence-confinement method was utilized. In addition to the analytical analyses, 2D and 3D FEM analyses were also employed to control the validity of the

empirical support design and to determine the deformations and failure zones developed around the rock masses surrounding the tunnel. After installation of the support systems, the extent of the failure zones around the tunnel was generally reduced. The validity of the numerical simulations was checked using the convergence-confinement method. According to results obtained from convergence-confinement and 3D numerical modeling, the maximum deformation values are almost similar. Therefore, it was concluded that the empirical support recommendations were generally satisfactory and 3D FEM analysis gives the best solution in tunnel support design compared to 2D FEM analysis.

Consequently, as a significant supplement of future research work on this subject, it is suggested that the actual field monitoring data should be collected during the construction phase of the Salarha Tunnel for calibration of the numerical models and for controlling the validity of the proposed support system.

**Acknowledgements** The authors would like to express their sincerest gratitude to the editor and reviewers. Thanks are due to the Academic Writing and Translation Office of RTE University for improving the language of the manuscript. The authors gratefully acknowledge geological engineer Murat Konak from the Turkish General Directorate of Highways for the office work associated with this study.

## References

- Agan C (2016) Prediction of squeezing potential of rock masses around the Suruc water tunnel. *Bull Eng Geol Environ* 75(2):451–468
- Akgun H, Muratli S, Kockar MK (2014) Geotechnical investigations and preliminary support design for the Gecilmez tunnel: a case study along the Black Sea coastal highway, Giresun, northern Turkey. *Tun Und Space Tech* 40:277–299
- Aydan O, Akagi T, Kawamoto T (1993) The squeezing potential of rocks around tunnels; theory and prediction, *rock Mech. Rock Eng* 26(2): 137–163



- Barla G, Einstein H, Kovari K (2013) Manuscripts using numerical discrete element methods, rock Mech. Rock Eng 46(4):655
- Barton N (2002) Some new Q-value correlations to assist in site characterization and tunnel design. Int J Rock Mech Min Sci 39:185–216
- Barton NR, Lien R, Lunde J (1974) Engineering classification of rock masses for the design of tunnel support. Rock Mech 4:189–239
- Barton N, By TL, Chryssanthakis P, Tunbridge L, Kristiansen J, Loset F, Bhasin RK, Westerdahl H, Vik G (1994) Predicted and measured performance of the 62-m span Norwegian-Olympic-ice-hockey-cavern at Gjovik. Int J Rock Mech Min Sci Geomech Abstr 31(6):617–641
- Basarir H (2006) Engineering geological studies and tunnel support design at Sulakyurt dam site, Turkey. Eng Geol 86:225–237
- Basarir H (2008) Analysis of rock-support interaction using numerical and multiple regression modeling. Can Geotech J 45:1–13
- Bhasin RK, Barton N, Grimstad E, Chryssanthakis P, Shende FP (1996) Comparison of predicted and measured performance of a large cavern in the Himalayas. Int J Rock Mech Min Sci 33(6):607–626
- Bieniawski ZT (1974) Geomechanics classification of rock masses and its application in tunneling, Proceedings of the Third International Congress on Rock Mechanics, Vol. 1A. International Society of Rock Mechanics, Denver, 27–32
- Bieniawski ZT (1989) Engineering rock mass classifications. Wiley, New York, p 251
- Boon CW, Houlisby GT, Utili S (2015) Designing tunnel support in jointed rock masses via the DEM, rock Mec. Rock Eng 48(2):603–632
- Brown ET, Bray JW, Ladanyi B, Hoek E (1983) Ground response curves for rock tunnels. J Geotech Eng 109(1):15–39
- Cai M, Kaiser PK, Tasaka Y, Minami M (2007) Determination of residual strength parameters of jointed rock masses using the GSI system. Int J Rock Mech Min Sci 4(2):247–265
- Carranza-Torres C (2004) Elasto-plastic solution of tunnel problems using the generalized form of the Hoek–Brown failure criterion. In: Hudson, J.A., Xia-Ting, F. (eds.), Proceedings of ISRM SINOROCK 2004 Symposium, China. Int J Rock Mech Min Sci 41(3):480–481
- Carranza-Torres C (2009) Analytical and numerical study of the mechanics of rockbolt reinforcement around tunnels in rock masses, rock Mech. Rock Eng 42(2):175–228
- Carranza-Torres C, Diederichs M (2009) Mechanical analysis of a circular liner with particular reference to composite supports. For example, liners consisting of shotcrete and steel sets, Tun. Und. Space Tech 24:506–532
- Carranza-Torres C, Engen M (2017) The support characteristic curve for blocked steel sets in the convergence-confinement method of tunnel support design. Tun Und Space Tech 69:233–244
- Carranza-Torres C, Fairhurst C (1999) The elasto-plastic response of underground excavations in rock masses that satisfy the Hoek–Brown failure criterion. Int J Rock Mech Min Sci 36(6):777–809
- Carranza-Torres C, Fairhurst C (2000) Application of the convergence-confinement method of tunnel design to rock-masses that satisfy the Hoek–Brown failure criterion. Tun Und Space Tech 15(2):187–213
- Curran JH, Hammah RE, Thamer EY (2003) A two dimensional approach for designing tunnel support in weak rock, proc. 56th Canadian Geotech. Conference. Winnebeg, Monibota
- Deere DU (1964) Technical description of rock cores for engineering purposed. Rock Mech Rock Eng 1:17–22
- Detournay E (1986) Elastoplastic model of a deep tunnel for a rock with variable dilatancy. Rock Mech Rock Eng 19:99–108
- Goh ATC, Zhang W, Zhang Y, Yang X, Xiang Y (2016) Determination of earth pressure balance tunnel-related maximum surface settlement: a multivariate adaptive regression splines approach. Bull Eng Geol Environ. <https://doi.org/10.1007/s10064-016-0937-8>
- Goh ATC, Zhang Y, Zhang R, Zhang W, Xiao Y (2017) Evaluating stability of underground entry-type excavations using multivariate adaptive regression splines and logistic regression. Tun Und Space Tech 70:148–154
- Goodman RE (1995) Block theory and its application. Geotechnique 45(3):383–423
- Gurocak Z (2011) Analyses of stability and support design for a diversion tunnel at the Kapikaya dam site, Turkey. Bull Eng Geol Environ 70(1):41–52
- Gurocak Z, Solanki P, Zaman MM (2007) Empirical and numerical analyses of support requirements for a diversion tunnel at the Boztepe dam site, eastern Turkey. Eng Geol 91:194–208
- Güven IH (1993) 1:250000-scaled geology and compilation of the eastern Pontide, general Directorate of Mineral Research and Exploration (MTA) of Turkey, Ankara (unpublished)
- Hoek E (2007) Practical rock engineering, Evert Hoek consulting engineer Inc., Vancouver, Canada (available for download at). <https://www.rocsience.com/learning/hoek-s-corner/books>
- Hoek E, Brown ET (1978) Trends in relationship between measured in-situ stresses and depth. Int J Rock Mech Min Sci Geomech Abstr 15: 211–215
- Hoek E, Brown ET (1997) Practical estimates of rock mass strength. Int J Rock Mech Min Sci 34(8):1165–1186
- Hoek E, Diederichs MS (2006) Empirical estimation of rock mass modulus. Int J Rock Mech Min Sci 43:203–215
- Hoek E, Marinos P (2000) Predicting tunnel squeezing, tunnels and tunneling international. part 1 – November 2000, part 2–December 2000
- Hoek E, Carranza-Torres C, Corkum B (2002) Hoek–Brown failure criterion-2002 edition, proceedings of NARMS-TAC2002. Mining Innovation and Technology, Toronto, Canada, pp 267–273
- Hoek E, Carter TG, Diederichs MS (2013) Quantification of the geological strength index chart, 47th US rock mechanics and Geomechanics symposium. USA, San Francisco
- ISRM (2007) The complete ISRM suggested methods for rock characterization, testing and monitoring: 1974-2006. International Society of Rock Mechanics Turkish National Group, Ankara, Turkey, 628
- Karakus M, Ozsan A, Basarir H (2007) Finite element analysis for the twin metro tunnel constructed in Ankara clay, Turkey. Bull Eng Geol Environ 66(1):71–79
- Kaya A, Bulut F (2013) Stability analyses of tunnels excavated in weak rock masses using empirical and numerical methods. J Geol Eng 37(2):103–116
- Kaya A, Bulut F, Alemdag S, Sayin A (2011) Analysis of support requirements for a tunnel portal in weak rock: a case study in Turkey. Sci Res Essay 6(31):6566–6583
- Ketin I (1966) Tectonic units of Anatolia. J Gen Direc Min Res Exp (MTA) 66:23–34
- KGM (2013) Specification for highway works (in Turkish). Turkish Ministry of Public Works. General Directorate of Highways, Ankara
- Korkmaz S, Gedik A (1988) Geology of the Rize-Findikli-Camlıhemsin area and petroleum occurrences. J Geotech Eng 32(33):5–15
- Lü Q, Sun HY, Low BK (2011) Reliability analysis of ground–support interaction in circular tunnels using the response surface method. Int J Rock Mech Min Sci 48:1329–1343
- Muir-Wood AM (1975) Circular tunnel in elastic ground. Geotechnique 25(1):115–127
- Ö-NORM B2203 (1994) Untertagebauarbeiten werkvertragsnorm. Österreichischer Normen, Österreich
- Ozsan A, Basarir H (2003) Support capacity estimation of a diversion tunnel in weak rock. Eng Geol 68:319–331
- Ozsan A, Basarir H, Yuceel S, Cucen O (2009) Engineering geological evaluation and preliminary support design for the metro extension tunnel, Ankara, Turkey. Bull Eng Geol Environ 68(3):397–408
- Park KH, Kim YJ (2006) Analytical solution for a circular opening in an elastic–brittle–plastic rock. Int J Rock Mech Min Sci 43:616–622
- Rocscience Inc. (2016a) RocData v5.0 rock, soil and discontinuity strength analysis, Toronto, Ontario, Canada, [www.rocsience.com](http://www.rocsience.com)
- Rocscience Inc. (2016b) RS<sup>3</sup> v1.0 3D finite element analysis for rock and soil, Toronto, Ontario, Canada, [www.rocsience.com](http://www.rocsience.com)

- Rocscience Inc. (2017) RS<sup>2</sup> v9.0 finite element analysis for excavations and slopes, Toronto, Ontario, Canada, [www.rocscience.com](http://www.rocscience.com)
- Sari D, Pasamehmetoglu AG (2004) Proposed support design, Kaletepe tunnel, Turkey. *Eng Geol* 72:201–216
- Satici O, Unver B (2015) Assessment of tunnel portal stability at jointed rock mass: a comparative case study. *Comput Geosci* 64:72–82
- Sheorey PR, Murali MG, Sinha A (2001) Influence of elastic constants on the horizontal in situ stress. *Int J Rock Mech Min Sci* 38(1):1211–1216
- Solak T (2009) Ground behaviour evaluation for tunnels in blocky rock masses. *Tun Und Space Tech* 24(3):323–330
- Vardakos SS, Gutierrez MS, Barton NR (2007) Back analysis of Shimizu tunnel no. 3 by distinct element modelling. *Tun Und Space Tech* 22(4):401–413
- Wang Y (1996) Ground response of circular tunnel in poorly consolidated rock. *J Geotech. Eng* 122:703–708
- Wang HN, Utili S, Jiang MJ (2014) An analytical approach for the sequential excavation of axisymmetric lined tunnels in viscoelastic rock. *Int J Rock Mech Min Sci* 68:85–106
- Yalcin E, Gurocak Z, Ghabchi R, Zaman M (2015) Numerical analysis for a realistic support design: case study of the Komurhan tunnel in eastern Turkey. *Int J Geomech*. [https://doi.org/10.1061/\(ASCE\)GM.1943-5622.0000564](https://doi.org/10.1061/(ASCE)GM.1943-5622.0000564)
- Zhang W, Goh ATC (2012) Reliability assessment on ultimate and serviceability limit states and determination of critical factor of safety for underground rock caverns. *Tun Und Space Tech* 32:221–230
- Zhang W, Goh ATC (2015) Numerical study of pillar stresses and interaction effects for twin rock caverns. *Int J Numer Anal Methods Geomech* 39:193–206